A low-temperature specific heat study of giant dielectric constant materials

2008 J. Phys.: Condens. Matter 20 285214

(http://iopscience.iop.org/0953-8984/20/28/285214)

J. Phys.: Condens. Matter **20** (2008) 285214 (5pp) doi:10.1088/0953-8984/20/28/285214

A low-temperature specific heat study of giant dielectric constant materials

C P Sun[1], Jianjun Liu[2,3], J-Y Lin[4], Chun-gang Duan[3,5], W N Mei[2,3] and H D Yang[1,6]

[1] Department of Physics, Center for Nanoscience and Nanotechnology, National Sun Yat-Sen University, Kaoshiung 804, Taiwan, Republic of China
[2] Department of Physics, University of Nebraska at Omaha, NE 68182-0266, USA
[3] Nebraska Center for Materials and Nanoscience, University of Nebraska-Lincoln, Lincoln, NE 68588, USA
[4] Institute of Physics, National Chiao-Tung University, Hsinchu 300, Taiwan, Republic of China
[5] Department of Physics, University of Nebraska-Lincoln, Lincoln, NE 68588, USA

E-mail: yang@mail.phys.nsysu.edu.tw

Received 9 April 2008, in final form 29 May 2008
Published 17 June 2008
Online at stacks.iop.org/JPhysCM/20/285214

Abstract

A low-temperature specific heat study has been performed on the insulating giant dielectric constant material $CaCu_3Ti_4O_{12}$ and two related compounds, $Bi_{2/3}Cu_3Ti_4O_{12}$ and $La_{0.5}Na_{0.5}Cu_3Ti_4O_{12}$, from 0.6 to 10 K. From analyzing the specific heat data in a very low-temperature range, 0.6–1.5 K, and moderately low-temperature range, 1.5–5 K, in addition to the expected Debye terms, we observed significant contributions originating from the linear and Einstein terms, which we attributed as the manifestation of low-lying elementary excitations due to lattice vibrations occurring at the grain boundaries and induced by local defects. Together with the findings on electronic and mechanical properties, a phenomenological model is proposed to explain the high dielectric constant behavior in both low and high frequency regions.

(Some figures in this article are in colour only in the electronic version)

$CaCu_3Ti_4O_{12}$ (CCTO) and related compounds have attracted much attention because of its extraordinary dielectric behavior. The ceramic samples were first found to have a gigantic dielectric constant (K, up to 10^4) independent of frequency and temperature in the range of DC-10^5 Hz and 100–600 K, dropping steadily down to about 100 at 10^6 Hz and then remaining constant until high frequency $\sim 10^9$ Hz [1, 2]. A giant value of 10^5 was later reported in a CCTO single crystal; yet twin and domains still existed [3].

Usually, a large dielectric constant results from atomic displacements in a non-centrosymmetric structure near its phase transition temperature, e.g. in a ferroelectric. However, CCTO is of body-centered cubic perovskite structure, no deformations associated with dipole formation and no soft modes in the phonon spectra down to 35 K [4, 5] have been noted. In addition, the values of the dielectric constant seem to be dependent upon the preparation methods and post treatments of the ceramic samples [6, 7]. Many experiments on thin-film single crystal samples only had values about 100 [8]. In addition there is a group of single crystal and polycrystalline metal oxide samples with rock salt and fluorite structures, such as MnO, CoO [9], ZrO_2 and HfO_2 [10], which exhibit high dielectric constants $K \sim 25$–40. Extensive theoretical studies, including first principles calculations and lattice dynamics, have been performed on ZrO_2 and HfO_2, and the results agreed well with experiments.

A similar approach was applied to CCTO, the sub-IR frequency dielectric constants were estimated to be at most 70–80 [11, 12] when using the effective charges, static dielectric constant, and optical frequencies calculated from lattice dynamics of a perfect crystal. This is smaller than the high frequency dielectric constant, thus it is vital to examine the structural details of the samples.

Several proposals have been put forward that the high dielectric constant of CCTO could originate from the creation

[6] Author to whom any correspondence should be addressed.

of barrier layer capacitances at twin boundaries [1, 3], or at the interfaces between grains and grain boundaries [13, 14], or between the sample and the electrodes [2, 15]. Current–voltage measurements show that the grain boundaries in the ceramics samples play an important role in the CCTO electrical properties [16]. We have made an effort to characterize the temperature dependence of the permittivity and impedance of CCTO and related compounds such as $Bi_{2/3}Cu_3Ti_4O_{12}$, $La_{2/3}Cu_3Ti_4O_{12}$, and $Y_{2/3}Cu_3Ti_4O_{12}$ [14, 17]. We found that all these compounds have similar dielectric and electric behavior; i.e. they are insulators and all have large dielectric constants, though perhaps not as high as that of CCTO. In all these compounds we detected a Debye-like relaxation in the permittivity and frequency-dependent current/voltage measurements with dielectric constants independent of the temperature and frequency over a wide range. In the impedance frequency-dependent voltage/current measurements, we observed some evidence for two electric responses with very different intensity and response frequencies. One relates to the semiconducting grains and the other insulating grain boundaries that we ascribed to the Maxwell–Wagner relaxation of the interfacial polarization. These are due to oxygen deficiency occurring at the regions between grains and grain boundaries that generates the detected Debye-like relaxation and large dielectric constants.

Based on the impedance and scanning electron microscopy (SEM) studies (figure 1), we suggested [14, 17] a shell–core model where the ceramic samples consist of semiconducting grains partitioned from each other by poorly insulating grain boundaries. To establish this model as a source of the extraordinary dielectric behavior, we combined x-ray diffraction and high- pressure techniques [18] and found the ceramic CCTO samples behaved differently under the hydrostatic and uniaxial compression condition, which we explained in terms of the same model as samples being composed of grains with shells stiffer than the cores. Recently, a study [19] utilizing x-ray spectroscopy techniques provided another support to this scenario, and a new high-K material $K_xTi_yNi_{1-x-y}O$ was also well described using the insulating grain boundary model [20].

What now needs to be explored is the nature of the low-lying excitations of the microstructures in these high-K materials. This would offer us clues to unravel the origin the extraordinary dielectric behavior: it is well known that low-temperature specific heat data provides information for different elementary excitations of the ground state. The specific heat data can contain several independent contributions, such as electronic, magnetic ordering contributions, and lattice vibrations that are derived from dispersion relations. The latter contributions are conventionally separated into two parts: the Debye and Einstein modes [19, 21–23] that relate to two issues of key interest pertinent to this study. First, at the interface region of the grain boundaries, it was proposed that there may exist *corrugated phonon modes* with an elementary excitation spectrum behaving as $\omega \sim k^2$, where ω and k are the frequency and wavevector, respectively. This mode was used to portray bending motion of the long-chain molecules [24], and bond angle vibration in the Cu–O plane

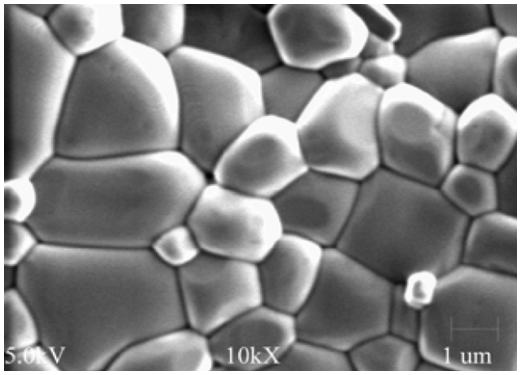

Figure 1. SEM image of the CCTO sample. Notice the grains are of the size of few microns, determined by using a JOELJSM840A scanning electron microscope set at 5 kV. The sample surfaces were gold-coated prior to examination.

of high T_c superconductors [25] due to the corrugation that the z coordinates of O and Cu are different, the z direction being perpendicular to the Cu–O planes, that is the Cu–O planes are not flat. Furthermore, there was a report that grain boundary layers of samples are Ti-rich and Cu-poor [19], in effect that would lead to a structure deviating from the perfect cubic lattice of CCTO then rendering the boundary layers to corrugate. Hence we anticipate it would offer a basis for the stiff insulating grain boundaries that are capable of sustaining large amounts of charge and facilitating the giant dielectric constant at low frequency region. Hence this mode could be used to support the existing theories [13–15] and profound features would emerge in the LTSH data. Second, low-lying optical modes caused by the lattice defects during fabrication might assist us in exploring the nature of those reasonably high dielectric constants in the higher frequency region (10^6–10^9 Hz), which are about 100 or higher [11, 12]. Because the evaluation of the sub-IR dielectric constant requires a summation of all the optical modes, especially those low energy localized modes, it is conceivable that these values would be enhanced as we could identify those low-lying modes caused by defects.

In this work, we performed low-temperature specific heat (LTSH) studies of CCTO and two other high-K compounds, from 0.6 to 10 K. Of the three high-K compounds, $Bi_{2/3}Cu_3Ti_4O_{12}$ contains 1/3 of vacancies while $La_{0.5}Na_{0.5}Cu_3Ti_4O_{12}$ is a mixture of equal amounts of La and Na ions, at the sites originally occupied by Ca ions in CCTO. These polycrystalline samples were prepared by heating mixed stoichiometric amounts of the oxides $CaCO_3$, CuO, and TiO_2 for CCTO or Na_2CO_3, La_2O_3, Bi_2O_3 when fabricating other compounds in an oxygen atmosphere at 1000 °C for 30 h and with intermediate grinding. The final samples were ground into powder and verified to be in a single phase by Scintag PADV powder x-ray diffractometer. The LTSH $C(T)$ was measured by using a ^{3}He heat-pulsed thermal relaxation calorimeter [21–23] whose essential method of calculating the heat capacity is to reach the thermal equilibrium of the sample and background in less than a characteristic time following the applied heat pulse. In figure 2, we present the specific heat data $C(T)$ of our samples after subtracting the addenda contribution

Table 1. Fitting parameters for the low-temperature specific heat data of $CaCu_3Ti_4O_{12}$. The equation we used is $C(T) = C_{hyp} + C_{linear} + C_{lattice} = A/T^2 + \Lambda T + \beta T^3 + \delta T^5 + D(T_E/T)^2 \exp(T_E/T)/[\exp(T_E/T) - 1]^2$ and the values in the parentheses are the error bars of the fit.

A (mJ K mol^{-1})	Λ (mJ mol^{-1} K^{-2})	β (mJ mol^{-1} K^{-4})	δ (mJ mol^{-1} K^{-6})	D (J mol^{-1} K^{-1})	T_E (K)	SD
1.2 (0.64)	0	0.559 (0.031)	0.0206 (0.0004)	0	0	16.30
1.27 (0.10)	0	0.489 (0.016)	0.0082 (0.0005)	9.0 (0.5)	53.8 (0.4)	0.46
0	2.32 (0.19)	0.259 (0.025)	0.0110 (0.0005)	7.0 (0.4)	50.7 (0.5)	0.43

Table 2. Best fitting parameters (same formula as table 1) for the three high-K compounds.

$ACu_3Ti_4O_{12}$	ε (f = 1 Hz)	A (mJ K mol^{-1})	Λ (mJ mol^{-1} K^{-2})	β (mJ mol^{-1} K^{-4})	δ (mJ mol^{-1} K^{-6})	D (J mol^{-1} K^{-1})	T_E (K)	SD
$CaCu_3Ti_4O_{12}$	9340	0.74 (0.11)	1.45 (0.20)	0.343 (0.024)	0.0100 (0.0005)	7.6 (0.4)	51.8 (0.5)	0.29
$La_{0.5}Na_{0.5}Cu_3Ti_4O_{12}$	3560	1.63 (0.23)	6.67 (0.37)	0.906 (0.054)	0.0128 (0.0007)	6.7 (0.3)	43.2 (0.4)	1.35
$Bi_{2/3}Cu_3Ti_4O_{12}$	2150	0	22.85 (0.36)	2.730 (0.060)	0.0060 (0.0005)	4.2 (0.1)	39.5 (0.4)	1.39

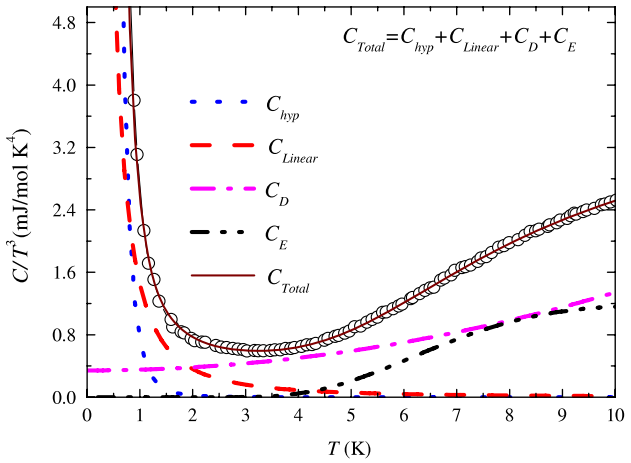

Figure 2. Low-temperature specific heat data (black circles), plotted as $C(T)/T^3$ versus T, from 0.6 to 10 K, and the best fit containing all the contributions is the solid line (SD = 0.29).

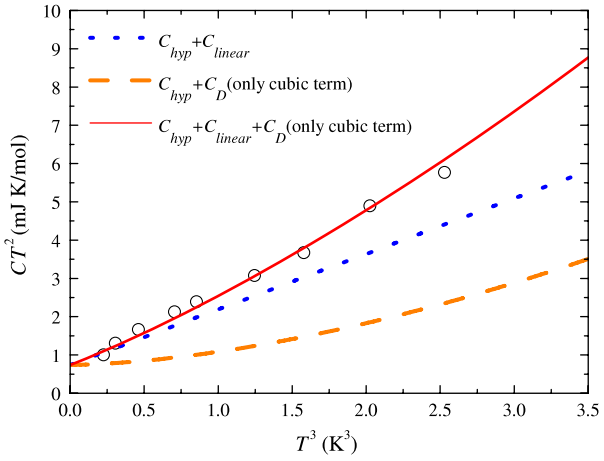

Figure 3. Specific heat data, plotted as $C(T)T^2$ versus T^3, from 0.6 to 1.5 K, and different fits: the model contains (i) C_{hyp} and C_{linear} is the dotted line, (ii) C_{hyp} and C_D is the dashed line, and (iii) C_{hyp}, C_{linear}, and C_D is the solid line.

determined from a separate measurement. In order to classify different contributions in the LTSH data, we fit the data by using the equation $C(T) = C_{hyp} + C_{linear} + C_{lattice}$ [26], where C_{hyp} is the hyperfine contribution ($\sim 1/T^2$) appearing in the lowest temperature region and is caused by the interaction between the crystal field and nuclear magnetic moments, such as those from Cu ($A = 63$) with 69% abundance and magnetic moment 2.2 μ_B. C_{linear} is a linear T term normally originating from the free electrons, and $C_{lattice} = C_D + C_E$ corresponds to Debye and Einstein modes, where $C_D = \beta T^3 + \delta T^5$ includes a linear frequency dispersion at low energy and an anharmonic term of lattice vibration, where β depends on the Debye temperature and atom number per unit cell, and might contain the contribution of the antiferromagnetic magnon with Neel temperature $T_N \sim 25$ K, because they have the same temperature dependence of specific heat. Moreover, C_E is caused by the low-lying dispersionless optical modes given as $C_E = D(T_E/T)^2 \exp(T_E/T)/[\exp(T_E/T) - 1]^2$, where D relates to the Einstein temperature T_E and number of Einstein modes per unit cell. In tables 1 and 2, we listed the acceptable fits: the parameters are positive, within a reasonable range and the standard deviations (SD) are small.

Since the three samples studied share similar characteristics, we choose to focus first on the CCTO results. After careful examination, we noticed two interesting features: (1) the appearance of Einstein modes at a low-temperature range $T < 5$ K and (2) the manifestation of a linear term in this good insulator ($\sim$0.45 MΩ cm at room temperature [11], similar for other reports and samples). Starting by analyzing the LTSH data using known contributions, we found that it was impossible to omit C_E and C_{linear}. The standard deviation for the best fit 16.30 could be obtained without incorporating linear and Einstein terms. But after we added C_E, SD decreased immediately to 0.46. Then by adding C_{linear}, values of the standard deviation dropped down to around 0.3. In figure 2, the entire low-temperature (0.6–10 K) specific heat data is shown together with the best fit including all the contributions. Later, in order to evaluate the relative merits between C_{hyp}, C_D and C_E contributions, we present the data as following: in figure 3, we notice that in the plot of $C(T)T^2$ versus T^3 in the lowest

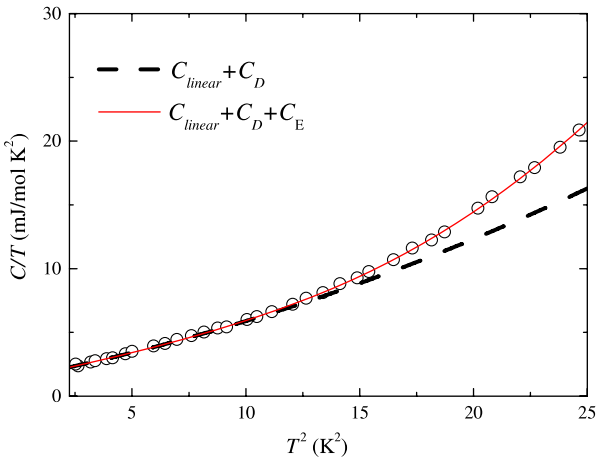

Figure 4. Specific heat data, plotted as $C(T)/T$ versus T^2, from 1.5 to 5 K, and different fits: the model contains (i) $C_{\rm linear}$ and $C_{\rm D}$ terms is the dashed line, (ii) $C_{\rm linear}$, $C_{\rm D}$ and $C_{\rm E}$ terms is the solid line.

temperature region from 0.6 to 1.5 K, we observe clearly that $C_{\rm hyp} + C_{\rm linear}$ describes the data better than $C_{\rm hyp} + C_{\rm D}$ (cubic term only). Finally, when combining the three terms, we reached a satisfactory agreement. Then in figure 4, we plotted $C(T)/T$ versus T^2 from 1.5 to 5 K. We would like to emphasize that $C_{\rm E}$ starts to rise above $C_{\rm linear}+C_{\rm D}$ around 3–4 K. Thus, from the above analysis, we deduce that there are other excitations on top of the Debye term that originate from the conventional acoustical modes. We know well the linear T term used to connect with the conduction electrons; however, CCTO is identified to be a good insulator. However, we observe sharp x-ray patterns that indicate our samples are in single phase, we thus correlate this linear T term in the low-temperature specific heat data with the *corrugated phonon modes* located at the grain boundaries as proposed earlier; and we deduce that the samples are composed of grains with tough shells that can be regarded as quasi-two-dimensional lattices. These corrugated phonon modes constitute the linear T term in the specific heat data. In addition, we find this picture matches with many existing theories [14, 17, 18]. Similar phenomena were reported in C_{60} studies [27], which were attributed to the disordered induced localized state but not a special feature in its excitation spectrum.

Usually, the Einstein term is related to the low-lying optical modes. According to the previous studies [11, 12], optical mode frequencies for the cubic phase CCTO ranged from 125 to 560 (cm^{-1}), so they are much higher than those observed in our specific heat data, in which the Einstein term started to appear about 3–4 K, around 2–5 (cm^{-1}). Thus, these modes are not generated from lattice vibrations of a perfect solid; rather they are expected to arise from local defects at the grain boundaries caused by oxygen deficiency inside the grains, which are produced during the heating process. Hence including these modes would increase the high frequency dielectric constants and provide an insight into the high dielectric constant at higher frequency as we expected.

In order to demonstrate that the above studied low-lying excitations are common in many similar materials, LTSH measurements and analysis of high-K materials such as $La_{0.5}Na_{0.5}Cu_3Ti_4O_{12}$ and $Bi_{2/3}Cu_3Ti_4O_{12}$ were carried out and compared with those of CCTO in table 2. We notice that contributions from the linear term are prominent in all the samples; CCTO is the smallest among them. This may imply that its grain boundary shell is the thinnest, and their Einstein temperatures $T_{\rm E}$ are of the same order of magnitude; yet CCTO is the largest among them, at this point it is our belief that more studies are needed to develop a reliable theory.

In conclusion, we present low-temperature specific heat studies on the giant dielectric constant material CCTO from 0.6 to 10 K. Clear indications of linear and Einstein term contributions were observed on top of the commonly detected Debye term that originated from the conventional acoustic phonons. We examined the data at different ranges, 0.6–1.5 K and 1.5–5 K, separately to stress their contributions. Similar results were obtained for other high-K materials such as $La_{0.5}Na_{0.5}Cu_3Ti_4O_{12}$, $Bi_{2/3}Cu_3Ti_4O_{12}$, and two distinct batches of CCTO with different oxygen pressure and baking temperatures, with only few per cent changes in the fitting coefficients. We found two main features in the low-temperature specific heat data: there are linear and Einstein contributions. We have reason to believe that the linear contribution to the specific heat at low temperatures is caused by the corrugated phonon modes. These phonon modes lead to stiff grain boundaries that are capable of holding large amounts of charge hence facilitating the observed low frequency high dielectric constants. Whereas the Einstein contributions suggest that the effects from the low energy optical modes, generated due to imperfections, is non-trivial and in turn provides an explanation for the origin of the high frequency high dielectric constants. Thus, combined with the previous theoretical and experimental studies on the electronic and mechanical properties of CCTO and the related high dielectric constant compounds, we put forward a phenomenological model consistent with many current theories that, in addition to the material, the microstructure and the associated elementary excitations are endemic to the high dielectric constant behavior.

Acknowledgments

We are grateful for the fruitful discussions with Professors Morrel H Cohen and Peter A Dowben. This work was partially supported by the National Science Council of Republic of China under contract NSC96-2112-M110-001 and the Nebraska Research Initiative.

References

[1] Subramanian M A, Li D, Duan N, Reisner B A and Sleight A W 2000 *J. Solid State Chem.* **151** 323
[2] Lunkenheimer P, Fichtl R, Ebbinghaus S G and Loidl A 2004 *Phys. Rev.* B **70** 172102
[3] Homes C C, Vogt T, Shapiro S M, Wakimoto S and Ramirez A P 2001 *Science* **293** 673
[4] Kolev N, Bontchev R P, Jacobson A J, Popov V N, Hadjiev V G, Litvinchuk A P and Iliev M N 2002 *Phys. Rev.* B **66** 132102

[5] Homes C C, Vogt T, Shapiro S M, Wakimoto S, Subramanian M A and Ramirez A P 2003 *Phys. Rev.* B **67** 092106
[6] Adams T B, Sinclair D C and West A R 2003 *Adv. Mater.* **14** 1321
[7] Bender B A and Pan M J 2005 *Mater. Sci. Eng.* B **117** 339
[8] Tselev A, Brooks C M, Anlage S M, Zheng H, Salamanca-Riba L, Ramesh R and Subramanian M A 2004 *Phys. Rev.* B **70** 144101
[9] Seehra M S and Helmick R E 1981 *Phys. Rev.* B **24** 5098
[10] Zhao X Y and Vanderbilt D 2002 *Phys. Rev.* B **65** 233106
[11] He L, Neaton J B, Cohen M H, Vanderbilt D and Homes C C 2002 *Phys. Rev.* B **65** 214112
[12] He L, Neaton J B, Vanderbilt D and Cohen M H 2003 *Phys. Rev.* B **67** 012103
[13] Sinclair D C, Adams T B, Morrison F D and West A R 2002 *Appl. Phys. Lett.* **80** 2153
[14] Liu J J, Duan C G, Yin W G, Mei W N, Smith R W and Hardy J R 2004 *Phys. Rev.* B **70** 144106
[15] Lunkenheimer P, Bobnar P V, Pronin A V, Ritus A I, Volkov A A and Loidl A 2002 *Phys. Rev.* B **66** 052105
[16] Chung G Y, Kim I D and Kang S J L 2004 *Nat. Mater.* **3** 774
[17] Liu J J, Duan C G, Mei W N, Smith R W and Hardy J R 2005 *J. Appl. Phys.* **98** 093703
[18] Ma Y Z, Liu J J, Gao C X, White A D, Mei W N and Rasty J 2006 *Appl. Phys. Lett.* **88** 191903
[19] Wang C, Zhang H Z, He P M and Cao G H 2007 *Appl. Phys. Lett.* **91** 052910
[20] Jana P K, Sarkar S, Chaudhuri B K and Sakata H 2007 *Appl. Phys. Lett.* **90** 242913
[21] Chen S J, Chang C F, Tsay H L, Yang H D and Lin J Y 1998 *Phys. Rev.* B **58** R14753
[22] Sun C P, Lin J Y, Mollah S, Ho P L, Yang H D, Hsu F C, Liao Y C and Wu M K 2004 *Phys. Rev.* B **70** 54519
[23] Yang H D, Lin J Y, Sun C P, Kang Y C, Huang C L, Takada K, Sasaki T, Sakurai H and Takayama-Muromachi E 2005 *Phys. Rev.* B **71** 20504
[24] Mei W N, Kohli M, Prohofsky E W and Van Zandt L L 1981 *Biopolymer* **20** 833
[25] Kang H, Cheng J P and Lee Y C 1989 *Phys. Rev.* B **40** 11410
[26] Phillips N E 1964 *Phys. Rev.* **134** A 385
[27] Beyermann W P, Hundley M F, Thompson J D, Diederich F N and Grüner G 1992 *Phys. Rev. Lett.* **68** 2046